TURBULENT EXPLOSIONS: A STUDY OF THE INFLUENCE OF THE OBSTACLE SCALE

H. Phylaktou, Y. Liu* and G.E. Andrews
Department of Fuel and Energy, University of Leeds, Leeds LS2 9JT
*Department of Safety Engineering, Taiyuan Institute of Machinery, Taiyuan, Shanxi, China

Synopsis
Most studies on turbulent explosions have been carried out at roughly constant turbulent length-scales and the suggested dependence on scale is based on very little systematic data. There is an uncertainty therefore, when extrapolating the findings from scaled tests (or small scale experiments) to full size applications. The present study was a methodical investigation of the influence of scale on turbulent methane/air explosions. The variation of scale was achieved by varying both the size of the explosion rig and the characteristic size of the obstacle (at a set rig size). The explosion test rigs were totally confined cylindrical vessels with diameters of 76, 162 and 500 mm and L/D ratios ranging form 4 to 22. The obstacles were perforated grid-plates with fixed blockage ratio and variable number of holes (and therefore variable length-scale of the induced turbulence). The characteristic obstacle scale ranged from 2 to 177 mm. The results indicate a much stronger dependence of turbulent burning velocity on the length scale than that suggested by existing correlations in the literature.

Key words
Turbulent explosions, obstacles, length-scale, explosion scaling

INTRODUCTION

Explosions in obstacle congested volumes are of concern to both the onshore process industries and to the offshore petroleum installations. Obstacles (in the form of process equipment, piping systems etc.) interact with the explosion-induced flow to generate turbulence which in turn interacts with the combustion process and causes a faster burning rate and a more severe explosion due to the resultant faster rate of pressure rise in the system. Therefore, for obstacle congested volumes increased protection measures are required (such as larger vent areas or faster suppression systems) to counter-balance the faster increase in pressure and keep the maximum pressure loading below damaging levels. Turbulent explosions (and turbulent combustion in general) are not well understood and for this reason, theoretical modelling of such explosion scenarios is not reliable.

Available turbulent combustion correlations are based on experimental data obtained under conditions of relatively low turbulent Reynolds numbers, typically well below 20,000. Explosion incidents in obstacle congested volumes are rarely characterised by turbulent Reynolds numbers below 70,000 and realistically, combustion in such events takes place in flows having Reynolds numbers of hundreds of thousands. It is therefore doubtful whether these correlations could be used for the prediction explosion behaviour in industrial layouts.

Another characteristic of the available correlations is the indicated small or no dependency of the turbulent burning velocity on the scale of turbulence. This uncertainty of the influence of length scale on turbulent combustion arises mainly because there has been no methodical investigation of this

parameter. In most studies the variation of the turbulent length scale has been a co-incidental side-effect of changing other variables. Usually each investigation of turbulent combustion has been carried out in a fixed geometry rig producing a characteristic length scale with small variation (dependent upon the conditions). Some variation of scale is obtained by comparison of different studies but considering the different measuring methods employed by the different research groups and the uncertainties associated with the measurements of turbulence levels, turbulent and laminar burning velocities, etc., it is clearly very difficult to isolate the influence of length scale. This problem is compounded by the fact that most of the studies have been carried out in similarly small scale rigs where the characteristic length scale rarely exceeded 40 mm and in the majority of cases it was below 10 mm (Abdel-Gayed and Bradley, 1981). The inadequacy of the scale of these experiments is immediately evident when compared to typical industrial scales which range from several tens of millimeters to several meters.

Field engineers base their predictive calculations of explosion overpressures on laboratory and field-scale experimental scaling studies. The technique of experimental scaling of explosions amounts to performing an experiment in a geometrically-equivalent, reduced-scale rig with the objective of reproducing the large scale overpressures and flame speeds in the reduced-scale set-up. To achieve this, it is necessary to compensate for the effects of smaller scale. In current practice this is done by increasing the reactivity of the mixture used at small-scale, either by using a more reactive fuel-gas (Taylor and Hirst, 1988) (ethylene as compared to methane for example) or by oxygen enrichment of the gas/air mixture (Catlin and Johnson, 1992). Potentially this technique can cater for any scenario, irrespective of complexity, and provide detailed characterisation of the explosion.

However, accuracy and success of the method depends heavily on the fundamental turbulent combustion model on which it is based. At present such models have been derived in small scale experiments with little or no variation of scale, and there are great differences not only on the reported dependence on scale (ℓ) but also on the dependence on other variables such as the laminar burning velocity (S_L), and the rms flow velocity (u'). In the absence of a proven and consistent turbulent combustion model it is unlikely that successful explosion scaling could be achieved (at present).

For a meaningful interpretation of results from small scale experiments and for application to real size explosion hazards the explicit influence of scale is required. The scale dependence may not be as important in applications where no large variation of scale is involved, as in engine combustion for example, but for explosion scaling where a scale factor of typically two or even three orders of magnitude is involved, then the dependence on scale is critical. However, as discussed earlier, information on the influence of scale is scant because most turbulent combustion studies have been carried out in fixed-size equipment. The present investigation was directed at this problem with the aim of providing data on the influence of a characteristic scale of the geometry on the burning rate of a propagating explosion. Single-hole and multi-hole grid plates were used as obstacles mounted in the path of a flame front moving axially in large L/D (length to diameter) cylindrical vessels.

Most investigators have studied the influence of obstacles using simple obstacle geometries such as wire meshes, tube arrays and perforated plates. These obstacle types although not representative (in a general sense) of industrial layouts permit easy investigation of the obstacle properties such as blockage ratio (BR), length scale, relative position, and degree of congestion; they also facilitate easy handling and mounting.

The majority of previous work has been of a qualitative rather than quantitative nature (reported quantitative data are not usually easily transferable to other systems), and the main parameters investigated were the effect of the blockage and of the degree of congestion on the flame propagation speeds. Most of the reported work was done in long tubes, generally open (at either one or both ends), with methane/air mixtures. A number of researchers (Mason and Wheeler, 1919; Chapman and Wheeler, 1926, 1927; Robinson and Wheeler, 1933; Schelkin, 1940; Evans *et al*, 1949) have shown that arrays of obstacles in such configurations greatly enhance the speed of flame propagation and can drastically reduce the transition distance to detonation. Other authors (Moen at al, 1980, 1982; Hjertager, 1983; Knystautas *et al*, 1984; Urtiew *et al*, 1983; Taylor, 1985, 1986) have also demonstrated that when the turbulence intensity is maintained by placing several obstacles in the path of a propagating flame, the rate of combustion and degree of turbulence become highly coupled so as to promote a strong feedback mechanism which in partly confined geometries can lead to violent explosions.

Few researchers have investigated the effect of baffles in long closed tube explosions. Kirkby and Wheeler (1931) used 10 orifice plate restrictions in the central part of a 1.7 m long 10 cm diameter closed tube. Strong flame acceleration was found with an almost instantaneous pressure rise once the flame reached the baffles. Starke and Roth (1989) presented a detailed investigation of the influence of a single obstacle on flame propagation in a short tube of an L/D of 3-5. In a low pressure explosion in a glass tube the blockage induced acceleration of the flame and its dependence on the blockage shape was clearly demonstrated. Detailed LDA measurements of the high jet gas velocities induced by the obstacle were presented.

Andrews and Herath (1988) presented data on the increase in the rate of pressure rise due to a four-hole obstacle in a long tube of L/D of 22 (the same rig was used in a large part of the present work). It was shown that the rate of pressure rise was a function of the obstacle blockage. The present authors (1991a) confirmed the strong dependence of the rate of pressure rise on the blockage ratio using a single-hole plate with varying blockage ratio (20 - 80 %). An additional finding of this work was that the single-hole obstacles induced higher rates of pressure rise than the 4-hole plates used by Andrews and Herath (1988) over the whole range of blockage ratios tested. This was probably due to the larger characteristic scale of the single hole obstacles.

The scale that is of relevance in turbulent combustion is not the overall size of the rig but the size of the "turbulence-generator" as this determines the turbulence length scale ℓ. In explosions the turbulence generators are the obstacles and for grid plate obstacles (or similar) the dimension that determines the length-scale of turbulence is the width of solid material between the holes, b (Baines and Peterson, 1951). It follows that if the blockage ratio (defined as the blocked area divided by the upstream flow area) of a grid-plate obstacle is kept constant while the number of holes is varied then the characteristic obstacle scale will also be varied. This was the principle used in the present experiments.

EXPERIMENTAL

The tests were carried out in three totally confined cylindrical vessels having diameters of 76, 162 and 500 mm (Rig 1, 2 and 3 respectively). The corresponding vessel lengths were 1.65, 3.0 and 2.0 m. The test rigs were constructed from 0.5-m-long flanged sections of steel tubing and were designed to withstand possible detonation pressures. Rig 1 was mounted vertically while the other two vessels were mounted horizontally. The flammable mixture (of either near stoichiometric (10%

v/v) or lean (6%) methane/air) was formed inside the vessel by partial pressures (to 1 atm) and mixed by recirculation. The mixture was then ignited with a spark at one of the vessel-end flanges (on the centre-line) - bottom end for the vertical vessel. The obstacles were 3 mm thick stainless steel grid-plates of nominal blockage ratio of 60% and these were mounted between the rig flanges. The obstacle position relative to the spark was such that the flame was allowed to complete the initial acceleration phase that is characteristic of large L/D explosions ignited at one end (Phylaktou et al, 1990; Phylaktou and Andrews, 1991b), before it encountered the obstacle. The obstacle position and other geometric details of the configurations tested are presented in Table 1.

Rig Characteristics			Obstacle position	Obstacle Characteristics				
Rig	D mm	L/D	X_{ob}/D	n_h	BR %	d mm	b' mm	b mm
1	76.2	21.6	6.8	1	60.0	48.2	26.7	28.0
				4	60.0	24.1	13.3	7.0
				16	60.0	12.0	6.7	3.5
				31	58.2	8.8	4.6	4.6
				76	59.4	5.6	3.0	3.0
				199	65.8	3.2	2.1	2.1
2	162.0	18.4	6.2	1	60.0	102.5	56.7	59.5
				4	60.0	51.2	28.4	14.9
				16	60.0	25.6	14.2	7.6
3	482.0	4.1	3	1	60.0	304.8/	168.7	177
				4	60.0	152.4	84.4	27
				9	60.0	101.6	56.2	23
				16	60.0	76.2	42.2	19

Table 1. Characteristic dimensions of the test-rig and obstacle configurations.(D=vessel internal diameter, L=vessel length, X_{ob}=obstacle distance from spark, n_h=number of holes, d=hole diameter, BR=blockage ratio, b'=average width of solid material between the holes, b=minimum width of solid material between the holes)

The characteristic length scale of the obstacle, b' is defined as the average width of the solid material between the holes. This variable is thought to control the size of the turbulent flow eddies produced downstream of the obstacle (Baines and Peterson 1951); this will be discussed more fully later. It can be shown that for a triangular array of holes b' is given by Eq. 1.

$$b' = 0.952\left(D\, n_h^{-0.5} - d\right) \qquad (1)$$

(symbols as in Table 1)

This equation was used to calculate b' for all plates used and it was found to give values comparable to the average measured width of blockage between the holes. In this calculation single hole obstacles were treated as part of an imaginary larger array of holes. The length scale b in Table 1 was the measured minimum width of the solid material between the holes and it was different from the average width, b', as defined above, particularly for the multihole obstacles.

In order to aid the discussion and the interpretation of the results that follow the characteristic scale of the obstacles tested (as listed in Table 1) were reconstructed in a graphical form in Fig. 1, as a function of the number of holes. Both scales (b' and b) are indicated in this figure. It will be shown that the experimental findings relate better to the minimum scale rather than the average (b rather than b').

Initially this study was intended to be limited to 1, 4 and 16 hole grid-plates at a fixed blockage ratio of 60% for all vessels. However, prompted by the results from these tests the investigation in Rig 1 was extended using 31, 76 and 199-hole grids that were made available from another application. The 31 and 76-hole plates had slightly lower blockage ratios (58.2 and 59.4%) respectively while the 199-hole plate had a blockage ratio of 65.8%.

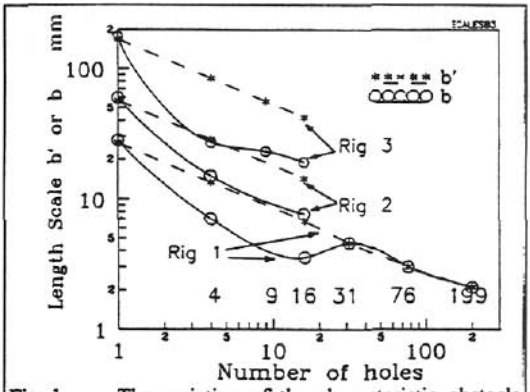

Fig. 1 The variation of the characteristic obstacle scale with the number of holes.

It is worth pointing out, at this point, the irregularity of variation of b between the 16-hole and the 31-hole grid-plates for Rig 1; the minimum width for the 31-hole plate was larger than that for the 16-hole grid (by about 1 mm or 25%). Also as indicated in Fig. 1, although the scales tested ranged from 2 to 177 mm the variation of scale between the 16-hole grid and the grids with larger number of holes was actually small in absolute terms -- 2-5 mm. It should also be noted that this scale, b, is not the same as the scale (ℓ) of the flow turbulence downstream of the obstacle. However, there is evidence that the turbulent length scale (ℓ) is related to the characteristic obstacle scale (b) and the distance downstream of the plate (Baines and Peterson, 1951). It should also be noted that (to the authors' knowledge) this is the first methodical investigation of the influence of length scale over such a wide range of scales.

An array of thermocouples along the axial centre-line of the vessel was used to record the flame-arrival time. This was detected as a distinct change in gradient of the analogue output of the thermocouple. The pressure variation was recorded using a SENSYM pressure transducer mounted at the centre of the flange at the far end from the ignition. Pressure drop measurements were also made across the obstacle and this enabled calculation of the explosion induced gas flow through the obstacle, ahead of the propagating flame. A fast (200 KHz), 34-channel, transient data acquisition system was used to record and analyse the data. Each test was repeated at least 3 times and averaged readings were used.

SOME GENERAL FEATURES OF THE EFFECT OF OBSTACLES

The effect of the obstacle in an explosion was assessed by comparison to the equivalent unobstructed explosion in the same vessel. The study of the empty-tube (no obstacle) explosions has been presented in detail by the authors (Phylaktou et al, 1990; Phylaktou & Andrews, 1991b) while the influence of single-hole obstacles of variable blockage has been reported in other publications (Phylaktou & Andrews, 1991 a, c; Phylaktou, 1993). The most important characteristic of the

unobstructed explosions was shown to be the initial phase of rapid flame acceleration along the axis of the tube, associated with high rates of pressure rise. It was shown that this fast phase plays an important role in explosions with obstacles as well. The fast flame propagation and the high combustion rates push the unburnt gas ahead of the flame at high velocities. The interaction of this unburnt gas flow with an obstacle and the coupling with combustion was shown to result in the combustion rates being enhanced by a factor of over a 100 for high blockage ratios and the right baffle positioning. In qualitative terms the presence of the obstacle was found to result in increased flame speeds, higher rates of pressure rise, reduced total combustion times, and in general higher maximum pressures.

These points are illustrated in Fig. 2, (a) and (b), for a slow burning, 6% methane/air mixture. Figure 2(a) compares a pressure-time signal without a baffle to that with a single-hole, 70% blockage at 6.8 diameters from the spark. The pressure curve with the baffle in position showed two consecutive steep pressure rises which brought the pressure in the vessel to about 65% of its maximum value in the initial 15% of the total explosion time. The first rate of pressure rise, $(dP/dt)_1$ as marked in Fig. 2(a), was the same (both in magnitude and timing) as that observed in the tube without any obstacles and was due to the initial acceleration of the flame along the tube. The second, $(dP/dt)_2$, was due to the presence of the baffle, and it was significantly higher than the corresponding rate of pressure rise in the unobstructed tube. The axial flame position-time curve (x/D) (with the baffle) shows a similar rapid increase and a close correspondence to the pressure variation.

The flame speeds corresponding to the pressure signals of Fig. 2(a), are shown in Fig. 2(b) as a function of the dimensionless axial distance from the spark (x/D). The flame speed before the baffle was almost identical to the flame speed in the unrestricted tube. After the baffle, however, there was a large increase in the flame speed which reached a maximum value at some distance downstream of the obstacle and then

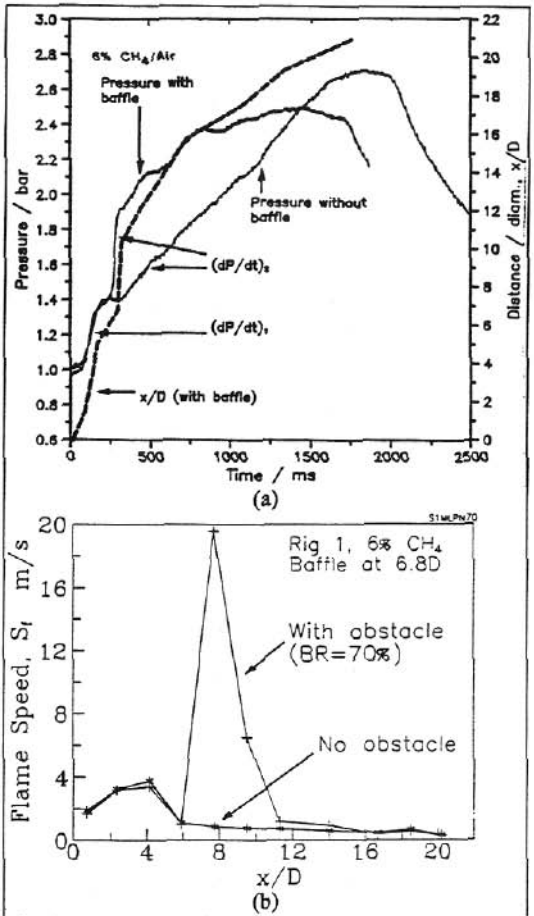

Fig. 2. (a) A typical example of pressure-time and distance-time curves for a 6% methane/air explosion with 70% blockage compared to the pressure signal without an obstacle.
(b)Corresponding flame speeds as a function of the dimensionless axial distance.

decayed to the "no obstacle" values towards the end of the vessel.

The accelerated flame propagation downstream of the obstacle and in particular the increased rate of pressure rise indicated that the mass burning rate (dm_b/dt) was enhanced when the flame reached this region. This enhancement was due to turbulent burning which in turn was caused by the ignition of the turbulent unburnt gas flow generated by the interaction of the explosion-induced flow with the obstacle whilst the flame-front was still on the upstream side. The flame-speed profile in the wake of the baffle corresponded to the profile of turbulence generated by steady-state flow through screens (Baines and Peterson, 1951) i.e. there was a development region, a maximum value at some distance from the obstacle, and a decay region (this is shown in Fig. 2(b) and will be illustrated more clearly in later figures). Since the flame-front is accelerated by turbulent combustion it could be argued that the relative increase in flame speed compared to the unobstructed test gives the relative increase in the burning velocity of the mixture due to turbulence. However, the flame speeds as measured in these experiments can only be used as a rough guide of the relative increase in burning rate because the flame speed record was non-continuous and one-dimensional, therefore not giving a true global picture of the effects of turbulence. It will be demonstrated later that the rate of pressure rise (dP/dt) is a much more reliable indicator of the increase in burning rate and in burning velocity.

Another example of pressure development and flame movement with the obstacle in position, using 10% methane/air mixture and a 16-hole 60% blockage, is shown in Fig. 3(b). This is compared to the equivalent unobstructed test, shown in Fig. 3(a). In similarity to the 6% methane/air tests, the pressure development and flame movement before the flame encountered the obstacle was not influenced much by the presence of the obstacle. However, downstream of the obstacle there was a considerable increase in both the rate of pressure rise (marked as $(dP/dt)_2$) and the rate of flame propagation as indicated by the x/D curve.

The burning rate enhancement due to the presence of the obstacle can be simply (qualitatively) demonstrated by consideration of the total explosion duration as marked by the flame arrival at the last thermocouple (represented by the last point on the x/D curve), or by the time when the pressure reached its maximum value. Figure 3 shows that the 16-hole plate reduced the explosion duration to under half that of the unobstructed test (from about 570 ms to about 240 ms), indicating that in overall

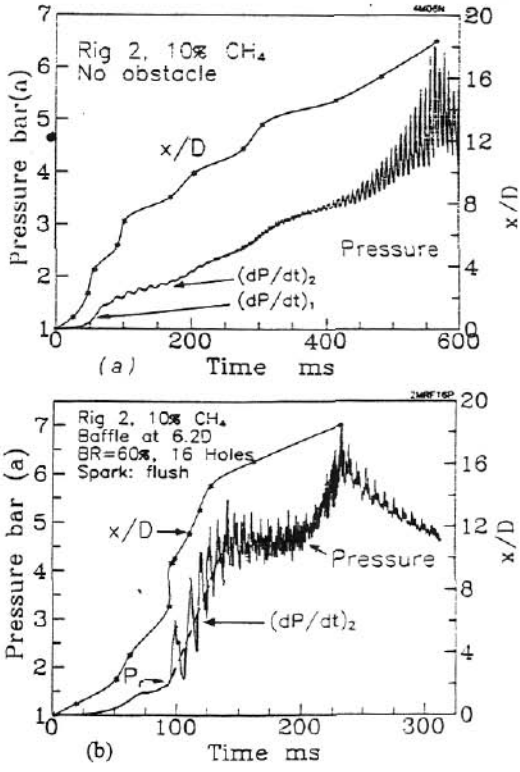

Fig. 3. Typical pressure-time and distance-time curves for a 10% methane air explosion in Rig 2 (a) without an obstacle (b) with a16-hole obstacle at 6.2D.

average terms the burning rate was more than doubled. However the maximum enhancement factor of the burning rate, in the region downstream of the obstacle, was much higher than 2, and comparison of the second rates of pressure rise $(dP/dt)_2$* for the obstructed and unobstructed explosions suggests an enhancement factor of about 15.

THEORY

The increase in the rate of pressure change (dP/dt) in the system was a much better measure of the change in the burning rate because the measurement of the pressure variation was continuous and by nature a materialisation of the overall, averaged effects of turbulent combustion, i.e. not representing localised fluctuations but global changes in the burning rate due to the root-mean-square (rms) *turbulent velocity. Considering the combustion of an initially quiescent gas/air mixture in a totally* confined vessel and using the procedure described by Harris (1983) it can be shown that:

$$V\left(\frac{dP}{dt}\right) = \frac{dm_b}{dt}\left[\frac{RT_b}{M_b} - \frac{RT_u}{M_u}\right] \qquad (2)$$

where, V is the volume of the vessel, dm_b/dt is the mass burning rate, R is the universal gas constant, M is the mean molecular weight and T is the temperature with subscripts b and u referring to "burnt" and "unburnt" species respectively. It is assumed that combustion takes place in a flame-front of negligible thickness, burnt and unburnt gases obey the perfect gas law, burnt gases attain equilibrium within negligible time and pressure is uniform throughout the vessel.

The mass burning rate is given by the general equation

$$dm_b/dt = A_f \rho_u S_u \qquad (3)$$

where A_f is the flame area, ρ_u is the unburnt gas density and S_u is the burning velocity (this could be either laminar (S_L) or turbulent (S_T)).

Changes in the burning velocity S_u would result in changes in the mass burning rate (dm_b/dt) --Eq. 3 -- and in a closed system these would manifest as changes in the rate of pressure rise -- Eq. 2 -- which is an experimentally readily measurable quantity. By combining Eqs. 2 and 3 and substituting the unburnt gas density in terms of the perfect gas law and introducing the expansion factor+, E , then the rate of pressure rise can be related to the burning velocity by

---

* The presence of severe pressure oscillations -- which for the present system were due to acoustic reasonance and have been studied and reported elsewhere (Phylaktou et al, 1990; Phylaktou, 1993) -- made the measurment of $(dP/dt)_2$ particularly difficult. As indicated in Fig. 3 this measurement was performed by drawing an imaginary average line through the pressure oscillations (effectively smoothing the oscillations out) and then measuring the slope of this line.

+ The expansion factor is defined as the ratio of unburnt to burnt gas densities and it can be shown to be given by

$$E = (T_b/T_u)(n_b/n_u)$$

where n is the number of moles.

$$\left(\frac{dP}{dt}\right) = \frac{A_f}{V} P(E-1) S_u \qquad (4)$$

Therefore, in a closed system the rate of pressure rise is directly proportional to the burning velocity of the mixture, and changes in the burning velocity, due for example to obstacle generated turbulence as in the present experiments, will be reflected in the easily measurable rate of pressure rise. Hence, (dP/dt) can be used to determine the variation of the burning velocity with the experimental conditions, and in the present case with the characteristic obstacle scale (b).

It should be emphasised that A_f refers to the bulk flame shape and not to the detailed structure of the flame front. The perturbations of the mean flame front are accounted-for in the definition of the turbulent burning velocity S_T (Damkohler, 1940). Some simplification to Eq. 4 could be achieved, if a dimensionless flame area function C_{Af} is defined, such that

$$C_{Af} = A_f / A_N \qquad (5)$$

where A_N is the minimum area normal to the direction of propagation. In the present experiments A_N was equal to the cross-sectional area of the tube (i.e. A_N=A). The value C_{Af} is dependent upon the flame shape downstream of the obstacle. For example C_{Af} would be equal to 1 for a planar flame-front shape and to 2 for a hemispherical shape. If in Eq. 4, A_f is expressed in terms of Eq. 5 (with A_N = A) and the volume is substituted as V = A L then the area A cancels out giving

$$\left(\frac{dP}{dt}\right) = \frac{C_{Af}}{L} P\,(E-1)\,S_T \qquad (6)$$

which indicates that for cylindrical vessels (dP/dt) is inversely proportional to the length of the vessel.

For a given geometry the maximum rate of pressure rise was recorded when the burning velocity, S_T , was at its maximum (and this in turn occurred when the flame ignited the region of maximum flow turbulence). The pressure P in Eq. 6 represents the mean pressure in the system at the time of maximum burning rate, and E is the effective expansion factor at the same time. The value of the pressure P was mainly influenced by the amount of mixture burnt by the time of the flame interaction with the obstacle and since for each vessel the obstacle position was fixed then the variation of P was minimal for each series of tests. The expansion factor E is mainly influenced by the burnt gas temperature which in turn depends on the heat loss rate from the system, and therefore for each vessel E was not expected to show appreciable test-to-test variation.

Since the objective of the present experiments was the determination of the influence of length-scale then any other influences had to be excluded from the experiments (or accounted for). The turbulent burning velocity S_T depends mainly on the maximum rms turbulent velocity u' of the flow, which in turn depends on the mean flow velocity upstream of the obstacle, and on the blockage ratio of the obstacle (Phylaktou & Andrews, 1991a). It is for this reason that the blockage ratio was kept nominally constant, while using the same combustible mixture for each series of tests was aimed at keeping the upstream flame speeds and thereby the induced flow velocity constant.

Therefore, on the basis of the theoretical analysis and the design of the experiment, it was expected that the variation of the rate of pressure rise with the obstacle-scale would reflect the dependence of the turbulent burning velocity on the length-scale of turbulence.

DEPENDENCE OF FLAME SPEED ON THE OBSTACLE SCALE

The variation of the centre-line flame speeds against the axial distance, with the different-hole obstacles in Rig 1 and Rig 2 are shown in Figs. 4 and 5 respectively. Both figures are divided into parts (a) and (b) for the 10 and 6% methane/air mixtures respectively. In all cases with exception of the 10% mixture in Rig 1 (Fig. 4(a)) the maximum flame speed downstream of the obstacle was obtained with the single hole obstacle and in general the maximum value decreased with increasing number of holes (decreasing b).

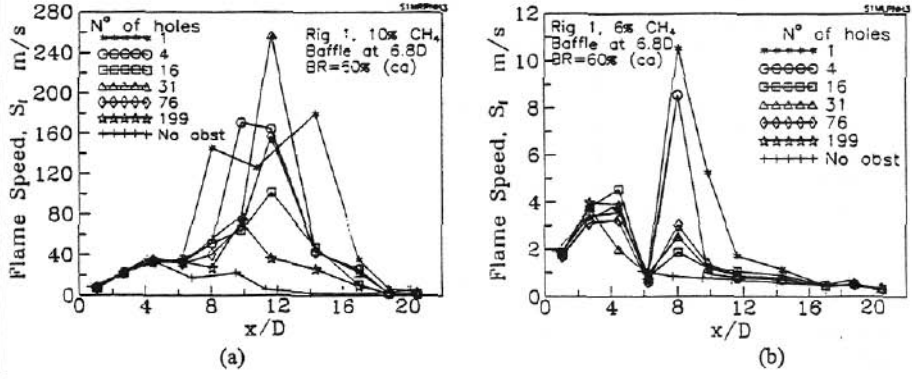

Fig. 4. Axial flame speeds in Rig 1 without and with an obstacle of variable number of holes (a) 10% methane/air (b) 6% methane/air

With the 10% mixture in Rig 1, Fig. 4(a), the maximum flame speed was obtained with the 31-hole obstacle. The flame speeds with the single-hole obstacle (BR=60%) in this rig were irregularly low, and it was shown elsewhere (Phylaktou & Andrews, 1991a) that the flame speeds for this obstacle were lower than the 40 and 50% single-hole blockages. It was also reported that for single hole blockages above 50% (for 10% methane/air mixtures) the flame was recorded to arrive at the second thermocouple downstream of the baffle after hitting the third thermocouple. This is thought to be due to localised turbulent flame quenching. In the calculation of the flame speeds for the single-hole obstacle in Fig. 4(a) this thermocouple reading was ignored and an average flame speed was calculated over a longer distance. This might have resulted in truncating the maximum flame speed downstream of this obstacle. This however does not explain why the "31-hole" flame speed was higher than that obtained with the 4-hole obstacle.

This behaviour of the 31-hole plate was not repeated with the 6% mixture as shown in Fig. 4(b). In fact the maximum flame speeds downstream of the 16-, 31- and 76-hole plates were similar, and this was a reflection of the similarity of the scale, b, for these 3 plates (see Fig. 1). On the basis of scale, the flame speeds downstream of the 31-hole grid should have been higher than those downstream of the 16-hole grid; they were in fact slightly lower and this might have been due to the lower flame speeds upstream of this obstacle, as shown in Fig. 4(b).

The dependence of the downstream flame acceleration on the upstream flame speed is almost linear (Phylaktou, 1993) and it derives from the upstream flame speed being the driving force behind the unburnt gas flow through the obstacle. The higher the upstream flame speed, the faster is the induced flow through the obstacle, the more intense is the turbulence downstream of the obstacle and the faster is the combustion rate and therefore the higher is the downstream flame acceleration.

As indicated in Fig. 4(b) the 6% methane/air explosion was not able to propagate through the 199-hole plate (this behaviour was consistent in repeated tests). This is thought to be due to flame quenching by flame-front beak-up and heat removal, which is a principle widely used in flame arrestors (traps). In order to propagate through this grid the flame had to be broken into small flamelets, of a size similar to the diameter d of the hole which was 3.2 mm. Furthermore, the aspect ratio (wall thickness/hole diameter) for this plate was equal to 1 and therefore the small weak flame had to propagate through what effectively was a small channel of heat absorbing metal. The heat loss rate for this flame must have been higher than the heat release rate and hence combustion was un-sustainable. The present results indicate that the quenching hole diameter for the 6% methane/air mixture is 3.2 mm or higher.

The flame speeds downstream of the 1-, 4-, and 16-hole obstacles in Rig 2 (shown in Fig. 5) followed (loosely) the trend of lower maximum flame speeds with lower scale obstacles. Another trend evident in this figure was that the flame speed peaked nearer to the obstacle with smaller scale obstacles. This observation is in agreement with the cold flow turbulence profile downstream of the obstacle, as reported in the literature (Baines & Peterson, 1951).

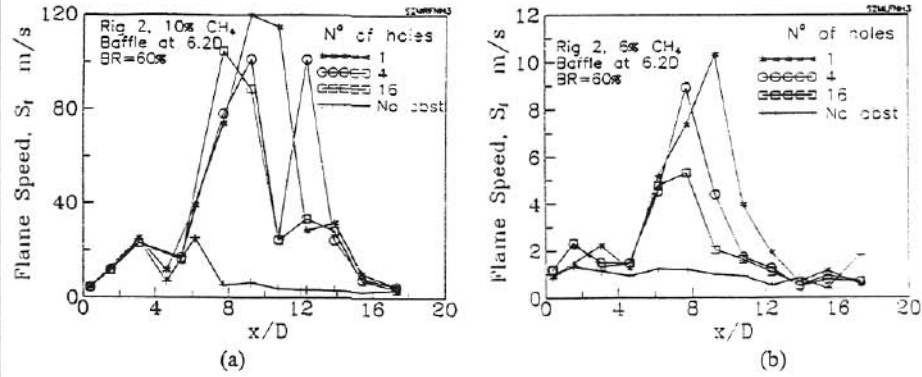

Fig. 5. Axial flame speeds in Rig 2 without and with an obstacle of variable number of holes (a) 10% methane/air (b) 6% methane/air

The 10% methane/air flame speeds in Rig 3 showed similar trends as in Rig 1 and 2. No 6% methane tests were carried out in this Rig because of complications due to buoyancy effects and it should be noted that the lean mixture results in Rig 2 were also distorted by this force. Because of the weakness of the mixture the buoyancy influences were comparatively strong. The horizontal orientation of vessels 2 and 3 also exacerbated these influences because the direction of action of buoyancy was vertical to the direction of flame propagation while in vertical-Rig 1 buoyancy was

acting in the direction of propagation. It is thought that with very lean mixtures in Rig 2 and 3, once the flame kernel started growing it was convected to the "roof" of the vessel and from there it spread along the vessel and downwards, resulting in stratified burning and in some cases "flash-over" because of the preheating (radiative and other) of the unburnt mixture. Although, no visual confirmation of this behaviour could be made there was experimental evidence to corroborate it (Phylaktou, 1993).

It should be emphasized that as indicated by Figures 4 and 5 the flame speeds downstream of the obstacle were not of the same value in the different vessels (for the same blockage and hole configuration). A number of factors were responsible for the different maximum flame speeds, including the upstream flame speed, and the system pressure at the time of the flame-obstacle interaction, as discussed earlier. The important finding which is fairly clearly demonstrated in Figs. 4 and 5 was that within a particular vessel and for the same mixture and blockage ratio the maximum flame speed downstream of the obstacle was reduced as the number of obstacle holes was increased (or as the characteristic obstacle scale was decreased).

DEPENDENCE OF RATE-OF-PRESSURE-RISE ON OBSTACLE SCALE

The rates of pressure rise downstream of the obstacle, $(dP/dt)_2$, are shown in Fig. 6 as function of the number of holes, for all conditions tested. In general the rate of pressure rise decreased with increasing number of holes with the exception of the tests with the 31-hole plate, for both the 10 and 6% mixtures, in Rig 1. $(dP/dt)_2$ with this plate was higher than that with the 16-hole plate. This apparent discrepancy was due to the fact that the characteristic scale b of the 31-hole plate was actually larger than that of the 16-hole one -- as shown in Fig. 1. The characteristic length of the 76-hole grid was similar to that of the 16-hole and this would explain the similar rates of pressure rise obtained with these grids with the 10% mixture but it does explain why the higher rate obtained with the 76-hole grid in the lean mixture tests. The rates of pressure rise in Rig 2 and Rig 3 decreased with increasing number of holes -- within the limited range of the tests.

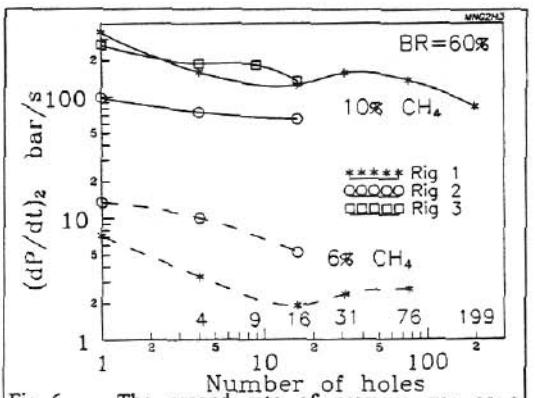

Fig. 6. The second rate of pressure rise as a function of the number of holes.

Therefore, there was a considerable decrease in the rates of pressure rise (indicating a decrease in the turbulent burning velocity) with increasing number of holes. Since, as shown in Fig. 1, increasing the number of holes decreased the characteristic scale of the obstacle, then it can be concluded that for a fixed blockage (within the individual rigs and for a particular explosive mixture) the rate of pressure rise increased with increasing obstacle scale. This trend was consistent for all three rigs and for both the explosive mixtures tested. This is demonstrated in Figs. 7(a) and 7(b) (for 10 and 6% methane/air respectively) where $(dP/dt)_2$ is plotted against the obstacle scale, b, for the different vessels employed.

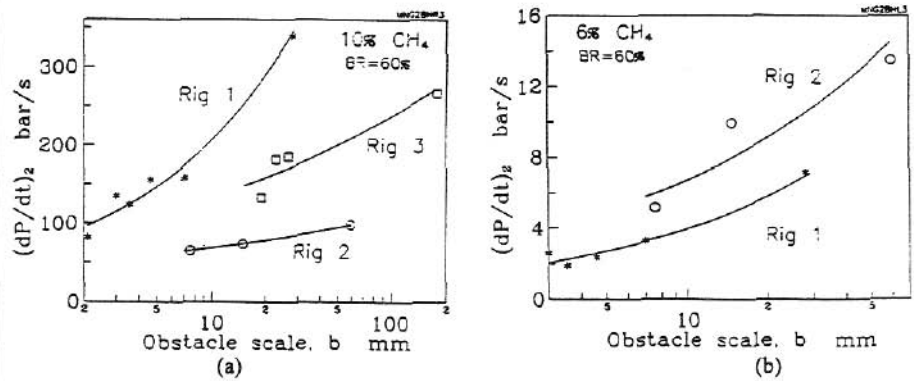

Fig. 7. The second rate of pressure rise as a function of the obstacle scale (a) 10% methane/air, (b) 6% methane/air.

The differences between the three rigs arose because of

a. different flame-area to vessel-volume ratios and in effect, as indicated by Eq. 6, different vessel lengths,
b. different pressures in the vessels at the time of the flame interaction with the obstacle, because of differences in the relative obstacle position,
c. different effective expansion ratios due to dissimilar heat loss rates resulting from different heat-exchange-area to volume ratios,
d. unlike flame speeds on the upstream side of the obstacle,
e. different frequency and amplitude of the pressure oscillations in the system which could have had significant influences on the combustion rate.

Some of the above parameters varied from test to test within the same rig, as well, but the magnitude of these variations was comparatively very small. Although it is possible to compensate for most of these differences and bring the data from the 3 test rigs together (Phylaktou, 1993) it is beyond the scope of this paper to do so, as a more detailed presentation of the results is needed, and validated development of methodology and procedure is required.

Figure 7 demonstrates, using fairly raw experimental data, the dependence of the rate of pressure rise (and hence of the turbulent burning velocity) on the characteristic obstacle scale. The results within each vessel were consistent and showed an increase of the turbulent burning velocity with the obstacle scale. This dependence is quantified by the least squares fitted curves to the data on Fig. 7. These fitted curves have the power form

$$(dP/dt)_2 \ (\propto S_T) \propto b^e \qquad (7)$$

which is the conventionally assumed dependence of S_T on scale. The value of the exponent e ranged from 0.2 to 0.54 with a mean value of 0.38, i.e.

$$(dP/dt)_2 \ (\propto S_T) \propto b^{0.38} \qquad (8)$$

with the standard deviation of the exponent being 40% (of the mean) and the standard error being 18%. The large uncertainty in the value of the exponent arises from the small number of samples, the unprocessed nature of the data, and from the statistical nature of turbulent combustion.

It should be remembered that the characteristic obstacle-scale b is directly related to the integral length-scale, ℓ of flow turbulence downstream of the obstacle. The dependence on ℓ indicated by Eq. 8 is significantly higher than that indicated by the turbulent combustion model of Bradley *et al* (1992) -- $\ell^{0.15}$ --but closer to the fundamental form of the fractal model -- $\ell^{0.26}$ (Gouldin, 1987). The accurate evaluation of the dependence of S_T on the length scale ℓ is of critical importance in scaling results from small scale tests to large scale applications. Both of the above models have been used to explore explosion scaling in congested volumes, the latter by Taylor and Hirst (1988) and the former by Catlin and Johnson (1992).

To demonstrate the importance of the scale dependence in explosion scaling, Table 2 compares the relative increase of flame speed and overpressure predicted by the different models as a result of a 20-fold increase in scale (which is a moderate scaling factor in explosion scaling practice). The flame speed is assumed to increase in proportion to the turbulent burning velocity, while the overpressure is taken as dependent on the square of the flame speed (Taylor and Hirst, 1988; Harris and Wickens, 1989).

Model	Bradley et al (1992)	Fractal	Present
Scale exponent	0.15	0.26	0.38
Flame speed factor	1.6	2.2	3.1
Overpressure factor	2.6	4.8	9.6

Table 2. Relative increase in flame speed and overpressure predicted by the different models as a result of a 20-fold increase in scale.

Although the difference on the dependence on scale indicated by the models is small in absolute terms, the resultant predictions particularly of overpressure are significantly different and could make the difference between safe and unsafe design. This underlines the need for more experimental data in order to determine with confidence the effects of scale.

CONCLUSIONS

The results from an experimental investigation of the influence of the characteristic obstacle scale in explosions were presented. The manifestations of the obstacle influence were identified to be mainly increased flame speeds and increased rates of pressure rise. For a totally confined explosion it was shown from theoretical considerations that the rate of pressure rise is directly related to the mass burning rate and to the turbulent burning velocity. By suitably designed experiments most other influences were eliminated and the effect of obstacle scale was methodically investigated over a wide range of values (2 to 177 mm). It was clearly demonstrated that the flame speed and the rate of pressure rise increased with increasing scale and assuming a power relationship of the form

$$S_T \propto b^e$$

the exponent e was evaluated to be about 0.38. This dependence on scale is higher than that indicated by other models which have been used in explosion scaling. Further analysis of the data is required to reduce the uncertainty in evaluating the exponent e and more experiments are needed over a wider range of scales.

The findings from this work show that the physical overall size of appropriate experiments does not have to be large or to be varied, only the turbulent length scale has to be varied (the experiment has to be larger than the larger turbulent length-scale that may be accommodated). This can be achieved within a fixed overall turbulent flow or explosion vessel by varying the size of the turbulence generating feature of the geometry. For example, grid plates in tubular geometries (as in the present experiments) offer a relatively easy way of methodically changing the length scale of turbulence by changing the number of holes on the grid for a fixed blockage, or the size of the tubes could be changed for a fixed grid-plate geometry. Both of these methods will change the characteristic obstacle size that controls the length-scale of the generated turbulence.

ACKNOWLEDGEMENTS

The authors would like to thank the Science and Engineering Research Council for funding this work and the British Council for funding Mr Liu's visit to Leeds.

REFERENCES

Abdel-Gayed, R.G. & Bradley, D., 1981, A two eddy theory of premixed turbulent flame propagation, Proc. R. Soc. Lond., A 301, p.1.

Andrews, G.E. & Herath, P., 1988, Influence of obstacles on the rate of pressure rise in closed vessel explosions, Progress in Aeronautics and Astronautics, Dynamics of Explosions (A.L Kuhl et al ed.), AIAA, 114, p.512. .

Baines, W.D. and Peterson, E.G., 1951, An investigation of flow through screens., Trans. ASME, 73, p.167.

Bradley, D., Lau, A.K.C. & Lawes, M., 1992, Flame stretch rate as a determinant of turbulent burning velocity, Phil. Trans. R. Soc. Lond., A 338, p.359.

Catlin, C.A. & Johnson, D.M., 1992, Experimental scaling of the flame acceleration phase of an explosion by changing fuel gas reactivity, Combustion and Flame, 88, p.15.

Chapman, W.R. and Wheeler, R.V., 1926, The propagation of flame in mixtures of methane and air. Part IV, J. Chem. Soc., p.2139 .

Chapman, W.R., and Wheeler, R.V., 1927, The propagation of flame in mixtures of methane air. Part V., J. Chem. Soc, p.758 .

Damkohler, G., 1940, The effect of turbulence on the flame velocity in gas mixtures, Z.F. Electrochem., 46, p.601, (English translation, NACA TM1112 (1947))

Gouldin, F.C., 1987, An application of fractals to modeling premixed turbulent flames, Combustion and Flame, 68, p.249.

Harris, R.J., 1983, The investigation and control of gas explosions in buildings and heating plant, British Gas, E. & F.N. Spon Ltd.

Harris, R.J. & Wickens, M.J., 1989, Understaning vapour cloud explosions - an experimental study, The Insttution of Gas Engineers, 55th Autumn Meeting, Communication 1408.

Hjertager, B.H., 1983, Influence of turbulence on gas explosions, Proc. Conf. on Control and Prevention of Gas Explosions, p.39.

Kirkby, W.A. and Wheeler, R.V., 1931, Explosions in closed cylinders. Part IV., J. Chem. Soc., p.2303.

Knystautas, R., Lee, J.H. and Chan, C.K., 1984, Turbulent flame propagation in obstacle filled tubes, Twentieth Symposium (International) on Combustion, The Combustion Institute, p.1663.

Mason, W. and Wheeler, R.V., 1920, The propagation of flame in mixtures of methane and air. J. Chem. Soc, 117, *(in two parts)* p.36, p.1227.

Moen, I.O, Lee, J.H.S., Hjertager, B.H., Fuhre, K. and Eckhoff, R.K., 1982, Pressure development due to turbulent flame propagation in large-scale methane-air explosions, Combust. and Flame, 47, p.31.

Moen, I.O., Donato, M., Krigst R. and Lee, J.H, 1980, Flame acceleration due to turbulence produced by obstacles, Combust. and Flame, 39, p.21.

Phylaktou, H., Andrews, G.E. and Herath, P., 1990, Fast flame speeds and rates of pressure rise in large L/D cylindrical enclosures, J. Loss Prev. Process Ind., 3, p.355.

Phylaktou, H. & Andrews, G.E., 1991a, The Acceleration of flame propagation in a tube by an obstacle, Combustion and Flame, 85, p.363.

Phylaktou, H. & Andrews, G.E., 1991b, Gas Explosions in long vessels, Combust Sci. and Tech., 77, p.27.

Phylaktou, H. & Andrews, G.E., 1991c, The effects of obstacles on enclosed gas explosions, Fire and explosion Hazards, The Inst. of Energy, p.63.

Phylaktou, H. 1993, Gas explosions in long closed vessels with obstacles. A turbulent combustion study applicable to industrial explosions, PhD Thesis, University of Leeds.

Phylaktou, H., Andrews, G.E., Mounter N. and Khamis, K.M., 1992, Spherical explosions aggravated by obstacles, IChemE Symposium series No 130.

Starke, R. and Roth, P., 1989, An experimental investigation of flame behavior during explosions in cylindrical enclosures with obstacles., Combustion and Flame, 75, p.111.

Taylor, P.H., 1985, Vapour cloud explosions - the directional blast wave from an elongated cloud with edge ignition, Comb. Sci. Tech., 44, p.207.

Taylor, P.H. & Hirst, W.J.S., 1988, The scaling of vapour cloud explosions: A fractal model for size and fuel type, 22nd Symposium (International) on Combustion.

Urtiew, P.A., Brandeis, J. and Hogan, W.J., 1983, Experimental study of flame propagation in semiconfined geometries with obstacles, Comb. Sci. Technol., 30, p.105.